PHILOSOPHICAL TRANSACTIONS OF THE ROYAL SOCIETY A MATHEMATICAL, PHYSICAL & ENGINEERING SCIENCES

Molecular Photoelectron Spectroscopy

D. W. Turner

Phil. Trans. R. Soc. Lond. A 1970 **268**, 7-31
doi: 10.1098/rsta.1970.0059

Phil. Trans. Roy. Soc. Lond. A. **268**, 7–31 (1970) [7]
Printed in Great Britain

Molecular photoelectron spectroscopy

By D. W. Turner
Physical Chemical Laboratory, University of Oxford

The principal features of helium 584 Å photoelectron spectra of molecular vapours are outlined. Factors affecting the number of bands observed and their relation to the number of occupied electronic energy levels are discussed. The effect of the molecular translational velocity on the fundamental line widths attainable is considered and is shown to be significant though generally small compared with the much more common line broadening arising from ionic decomposition. Sharp lines are often to be associated with the presence of classical lone pairs but exceptions are noted. Structural effects in the lone pair ionization of chloro- and bromo-compounds are indicated. Some evidence is given for a correlation between the change in vibrational frequency produced upon ionization and the difference between adiabatic and vertical ionization energies. The use of such a correlation in the analysis of vibrational fine structure is exemplified by considering the examples of methylfluoride, 1,1-difluoroethylene, sulphur hexafluoride, ketene and pyrazine. A comparison between the p.e. spectra of butadiene, acrolein and glyoxal is used to indicate the utility of the method in creating energy level diagrams for related series of compounds.

Photoionization and the formation of a photoelectron spectrum

Photons in the vacuum ultraviolet region of the spectrum whose energy is about 10 eV interact with atomic or molecular gases mainly to cause excitation, that is, to promote electrons to bound states even though there may be sufficient energy to cause ionization. The careful study of absorption spectra has however afforded many examples of regions of continuous absorption such as might be ascribed to immediate ejection of a free electron (Weissler 1956). Such a process has an oscillator strength f approaching unity but with a range of possible electron energies the photon absorption process may occur over a wide wavelength range. This usually results in the cross-section for the ionization at any particular wavelength being small compared with cross-sections for excitation where the whole oscillator strength is concentrated in much shorter wavelength range. Since continuous absorption may also arise from dissociation into molecular fragments or atoms;

$$\mathrm{M} \xrightarrow{h\nu} \mathrm{A}\cdot + \mathrm{B}\cdot,$$

the positive identification of the limits of a true ionization continuum is often uncertain.

Watanabe (1959) partially overcame the confusion between the many different modes of adsorption by restricting measurements to those in which only charged species were produced, i.e.

$$\mathrm{M} \xrightarrow{h\nu} \mathrm{A}^+ + \mathrm{B}^-, \tag{1}$$

or

$$\mathrm{M} \xrightarrow{h\nu} \mathrm{M}^+ + \mathrm{e}^- \quad \text{(initially)}. \tag{2}$$

Though no distinction between these two process is afforded the latter is usually the most common. His technique involved varying the wavelength of the light from a monochromator and observing the onset of the production of charged species in irradiated vapour by measuring the total current which can be passed between a pair of electrodes spanning the illuminated region.

In photoelectron spectroscopy we concern ourselves only with the processes which liberate electrons, i.e.

$$\mathrm{M} \xrightarrow{h\nu} \mathrm{M}^+ + \mathrm{e}^- \quad \text{(direct ionization)},$$

and possibly

$$\mathrm{M} \xrightarrow{h\nu} \mathrm{M}^* \xrightarrow{h\nu} \mathrm{M}^+ + \mathrm{e}^- \quad \text{(autoionization)},$$

where M^+ may be in a stable, meta-stable or unstable (repulsive) state.

Experimental methods for the energy analysis of slow electron beams have been fully discussed in the literature (cf. Klemperer 1965) and for the particular application to the present topic reference may be made to a forthcoming book (Turner 1970). Each spectrum shown here is a continuous record of electron count rate integrated over either 0.33, 1, or 3 s plotted as a function of electron kinetic energy. In the absence of a recognized convention for the plotting of photoelectron spectral curves we have adopted scales which relate most closely to the primary data. The ordinate scale of electron flux is in counts/second throughout and increases upwards and the abscissa scale of electron energy (E) increases from left to right. This latter choice requires some defence for the secondary, deduced data, ionization energy ($I = h\nu - E$) then increases from right to left contrary to, *inter alia*, the convention in mass spectroscopic literature. The arrangement we have chosen however is consistent with the English spectroscopic usage where wavelength increases from the left and so makes for easy comparison between photoelectron spectra and conventional optical spectra.

The helium resonance light source

In the first instance the use of the helium resonance line as a means of exciting photoelectron spectra in gases was inspired by two basic considerations. One of these was that most if not all of the valence shell levels in simple molecules might lie at energies greater than that of the helium resonance line at 584 Å ($h\nu = 21.2168$ eV), the other that ionization from each of these molecular orbital levels might be expected to be a fully allowed process. The early results (Turner & Al-Joboury 1962) seemed to confirm this rather general hypothesis and led to the adoption of certain 'guide lines' useful in the interpretation of the spectra observed. These we can enumerate as follows:

(*a*) The electron energies satisfy a modified Einstein relation:

$$E = h\nu - I_{1,2} - \Delta E_{\text{vib}} - \Delta E_{\text{rot}}.$$

(*b*) Koopmans's theorem holds.

(*c*) For molecules with only closed shells of electrons each orbital level is represented by an electron spectral band from (*a*) and (*b*) above, electrons of the same I_i but different ΔE_{vib} and ΔE_{rot} constitute a 'band'. Molecules with open shells however may give two or more bands for each occupied orbital level which can be ionized.

(*d*) The intensity of the electron flux in each band is related to the occupancy of each orbital energy level in the molecule (number of electrons having the same principal and azimuthal quantum numbers) and to the degeneracy of the ionic state produced after ionization. This intensity is expected to decrease as E increases since in general ionization cross sections decrease with increasing excess energy, at least for larger energies.

(*e*) Two electron ionization and Auger processes are excluded on energetic considerations.

It is clear that these guide lines are of significance only to the extent that their utilization aids the interpretation of complex spectra. They constitute a pattern of normal behaviour however, deviations from which are themselves significant and have attracted much attention recently.

Koopmans's theorem

Deviations from Koopmans's theorem in which the successive ionization potentials $I_{1,2,\ldots}$ are set equal to the negatives of the computed orbital energies ϵ can be exactly assessed only for the simpler molecules where satisfactory values of ϵ are obtainable. Deviations of several electronvolts are not uncommon but are liable to cause 'inversion' of order only for those levels whose energy differs by only 1 or 2 eV. Basch, Robin, Kuebler, Baker & Turner (1969) have been able to calculate Koopmans's theorem ionization potentials which tend to be rather uniformly high by about 8 % largely due to neglect of reorganization and electron correlation effects. This was shown to be adequate for the assignment of most of the photoelectron spectral bands in simple amides and carboxylic acids, and in certain small ring compounds. For nearly degenerate levels (difference in $\epsilon < 1$ eV) clearly great caution is necessary in invoking Koopmans's theorem. It should be possible to test Koopmans's theorem directly by seeking the p.e. spectrum of an electronically excited species. Oxygen $^1\Delta$ suggests itself since it is easily generated and has a long natural life but attempts to measure its spectra in detail have proved difficult (A. D. Baker, D. P. May & D. W. Turner, unpublished work).

The number of bands: the Franck–Condon principle in ionization

According to the Franck–Condon principle the transfer of excitation in an electronic transition occurs in a time which is short compared with that required for the execution of vibrational motion. It governs therefore in the present instance the relative probabilities of ionizing transitions from (usually) the molecular vibrational ground state ($v'' = 0$) to the various ionic vibrational states ($v' = 0, 1, \ldots$).

In the approximation of a transition moment, $G_{e'e''}$, which varies slowly with internuclear coordinates, r, the probability $P_{v'v''}$ is given by the Born Oppenheimer equation

$$P_{v'v''} = [G_{e'e''}]^2 \left[\int \psi_{v'} \psi_{v''} \, dr\right]^2.$$

The second squared term is referred to as the Franck–Condon factor and is directly proportional to $P_{v'v''}$ if $G_{e'e''}$ is constant.

The electron flux for each peak in a photoelectron spectrum showing resolved vibrational structure measures either directly or indirectly (see below) $P_{v'v''}$ at a particular energy (here 21.2 eV). Since for different vibrational levels v' the excess energy E $(= h\nu - I - E_{\text{vib}})$ is different $G_{e'e''}$ will not be a constant. It may however be expected to be only slowly varying where direct ionization is occurring. The array of peaks in the photoelectron spectrum is thus approximate in amplitude to the square of the Franck–Condon factors and their envelope to the so-called 'Franck–Condon envelope'.

The 'one band per orbital' (and vice versa) rule is then open to the objection that certain ionization processes yield bands whose contours do not have the simple form of Franck–Condon envelope which has a single maximum. This may arise either from a competition between alternative ionization pathways each favouring a different group of vibrational levels in the product ion or from the generation of the ion in alternative and potentially non-degenerate electronic states. The former process occurs when the exciting line $h\nu$ coincides with a strongly autoionizing absorption line in the target molecule and has so far only been clearly demonstrated by Price (1968) and Collin & Natalis (1968) using the neon resonance light source. It seems possible that the higher the primary photon energy the smaller is the probability of encountering such processes especially in larger molecules. The latter is a special case of the dynamic Jahn–Teller effect and is well seen in the case of allene (figure 1). Here ionization of one of the four electrons from the doubly degenerate π level leaves the ion initially in a symmetric geometrical configuration but in one of two ionic states which lose their degeneracy when a non-symmetric deformation occurs (Baker & Turner 1969). As Longuet-Higgins, Öpik, Pryce & Sack (1958) and his associates showed theoretically for optical excitation process complex vibrational fine structure with a double maximum is the consequence. Other examples are provided by the p.e. spectra of methane, ethane (Baker, Baker, Brundle & Turner 1968) and possibly also by the first two bands of cyclopropane (Basch *et al.* 1969) (figure 2*a*, *b*, *c*). The effect of course is limited to molecules of high symmetry.

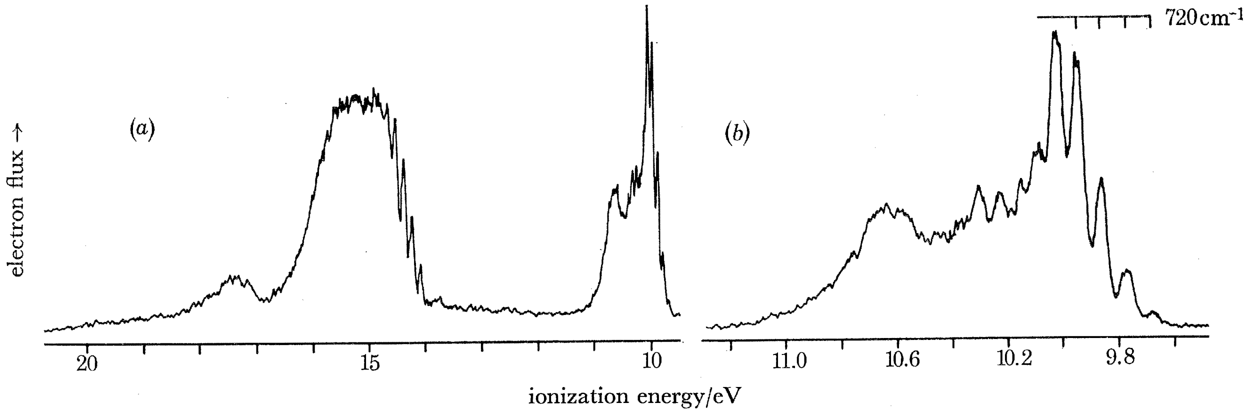

FIGURE 1. The helium 584 Å photoelectron spectrum of allene (*a*) and (*b*) the first band to an expanded abscissa scale.

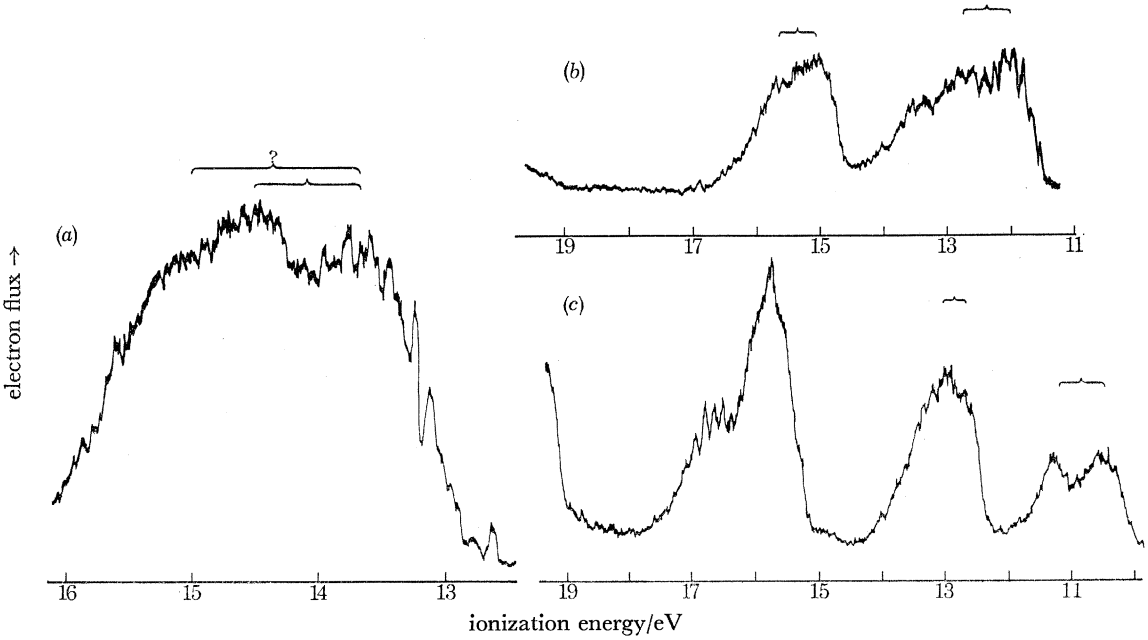

FIGURE 2. The helium 584 Å photoelectron spectra of (*a*) methane, (*b*) ethane and (*c*) cyclopropane.

Open-shell systems

When the photoelectron spectra of oxygen and nitric oxide were first obtained (cf. Al-Joboury, May & Turner 1965) the available resolution while revealing the presence of extensive vibrational fine structure in the second π ionizations was insufficient to show that it was in fact more complex than that required for assignment to a single long vibrational progression. Even the most recent experiments (Turner 1968) with much better apparatus still do not show this for oxygen where two states $^2\Pi_u$ and $^4\Pi_u$ are expected after loss of a $2p\pi_u$ electron. For nitric oxide however where six states are expected $^1\Sigma^+$, $^1\Sigma^-$, $^1\Delta$, $^3\Sigma^+$, $^3\Sigma^-$, $^3\Delta$ the overlap of different vibrational components is less and it is now possible with help from Lindholm's

PHILOSOPHICAL TRANSACTIONS OF THE ROYAL SOCIETY A MATHEMATICAL, PHYSICAL & ENGINEERING SCIENCES

evaluation of Rydberg series studies to locate five of the expected six bands (Lindholm, personal communication).

In the majority of substances the molecules are singlets in their ground states and such complexities may not be common except in the field of transition metal compounds where partly filled shells are the rule rather than the exception. Examples from this field are to be discussed by Dr M. L. H. Green in forthcoming papers.

Fine structure

If the photon energy were partitioned only between the kinetic energy of the ejected electron and electronic excitation in the ion the resultant spread in electron energies would be just that expected from the lifetime, τ of the ionic state according to the Heisenberg uncertainty principle. This natural line width must increase rapidly with the configurational energy stored in the ion, that is with the depth of the shell from which the electron is ejected.

For electrons ejected from the valence shell however $\tau \approx 10^{-8}$ s and the electron energy spread is sufficiently small (10^{-7} eV) so that the rather broad bands (up to 3 eV wide) often observed show the importance of other factors. These can be summarized as follows:

(*a*) The translational motion of the molecule before ionization contributes a small but, in light molecules, significant width.

(*b*) Some contribution from the light source line width may be expected in the case of sources where self reversal is very marked.

(*c*) Ionic vibration and fragmentation are, however, the dominant factors determining the band shape in valence shell photoelectron spectroscopy.

We shall consider (*a*) and (*c*) more closely. Samson (1969) has examined the contours of the helium resonance line (*b*) in some detail.

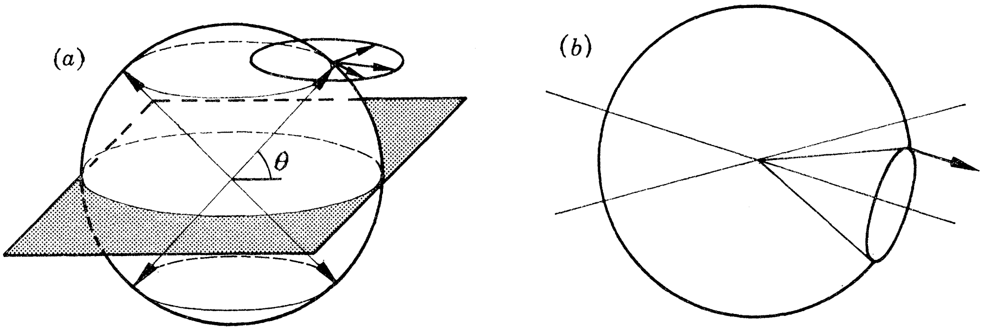

Figure 3. The combination of molecular velocities and electron velocities with respect to (*a*) a plane and (*b*) a preferred axis—see text.

Line broadening arising from the translational motion of the target molecules

The observed electron energies may range from $\frac{1}{2}M_e(v_e+v_m)^2$ to $\frac{1}{2}M_e(v_e-v_m)^2$ to give a total breadth of $2m_e v_e v_m$. Here v_m is the component of the most probable velocity (α in the Maxwell distribution $= (2kT/M)^{\frac{1}{2}}$) in the direction of motion of the electron as it enters the analyser. The most probable values that this component may take varies with the analyser geometry used.

In the cylindrical grid type of analyser the distribution of molecular velocities with respect to their angle (θ) from the plane normal to the incident light is important (figure 3*a*). The probability falls to 0.5 at $\theta = 60°$ at which angle the radial component of velocity ranges from $\alpha \cos\theta$ to $-\alpha\cos\theta$ depending on the relative azimuthal angles for electronic and molecular motion in the normal plane (figure 3*b*). The average radial component of the velocity is then in the range $\pm \frac{1}{2\sqrt{2}}\alpha$.

For an analyser which accepts electrons only close to a preferred axis distribution of molecular velocities with respect to the angle from this axis ϕ is important (figure 4*b*). The distribution has a half of its maximum probability at $\phi = 30°$ at which angle the axial velocity component range is $\pm \frac{1}{2}\sqrt{3}\,\alpha$.

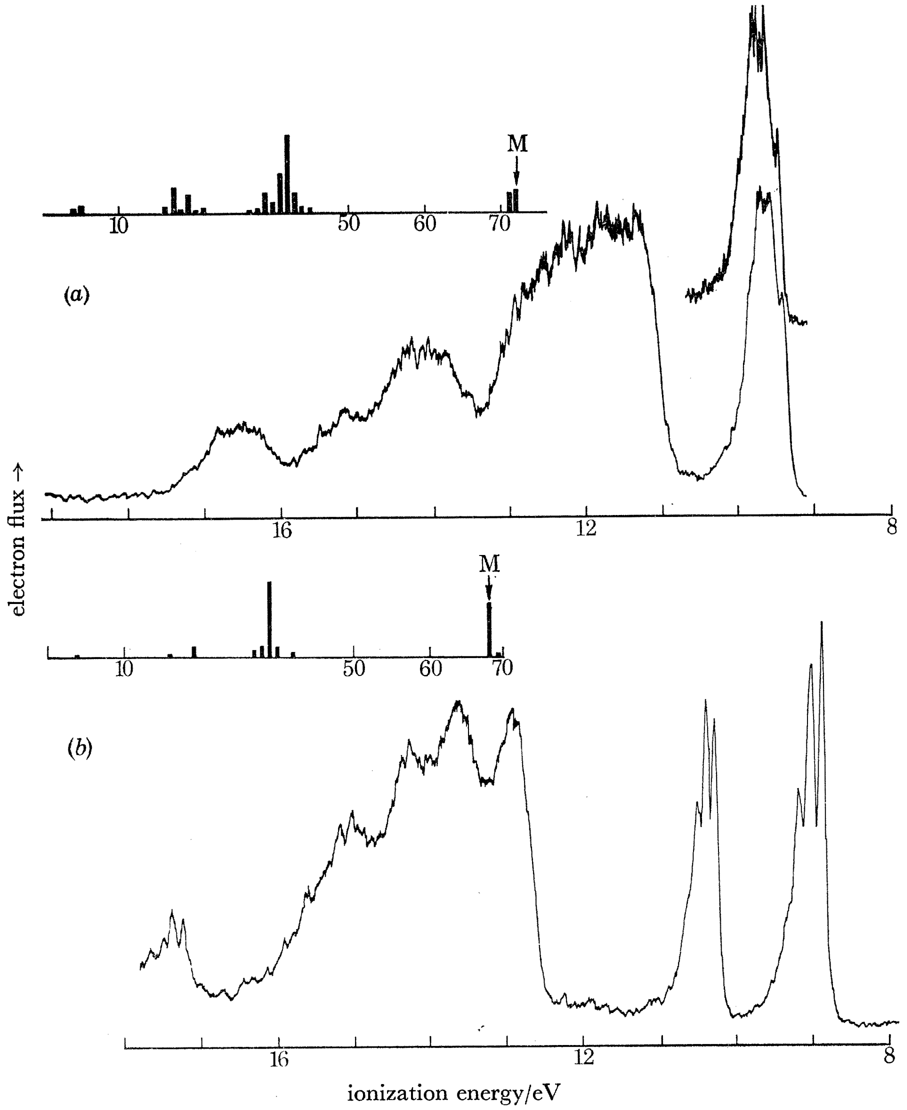

FIGURE 4. The helium 584 Å photoelectron spectrum and the electron impact mass spectrum of (*a*) tetrahydrofuran and (*b*) furan.

In these two cases therefore ΔE, the broadening expected is different:

$$\Delta E_{(\text{cylindrical retarding field})} = (2M_{\text{e}}kTE/M)^{\frac{1}{2}} = 0.306(ET/M)^{\frac{1}{2}}\,\text{mV},$$

$$\Delta E_{(\text{focusing analyser})} = (12M_{\text{e}}kTE/M)^{\frac{1}{2}} = 0.751(ET/M)^{\frac{1}{2}}\,\text{mV}.$$

Typically for $M = 100$ the broadening expected is 1.7 and 4.1 mV respectively for 10 eV electrons but increases to 17 and 41 mV for 1000 eV electrons. For hydrogen, ionized by $h\nu = 21.2$ eV photons broadening of 8.4 and 20.3 mV is expected in the two cases.

Line broadening arising from ionic decomposition

The molecules of complex organic and inorganic substances afford positive ions whose stability is often severely limited for quite small values of internal energy. Mass spectroscopy has provided a large body of data which indicate that in the majority of cases even a few electronvolts of internal energy suffices for the initiation of decomposition, a process for which the rate constants have been measured only in the range 10^7 to 10^5 s^{-1} but may extend to 10^{14} s^{-1} (immediate breakdown). Unstable ionic states cannot be characterized by precise ionization potentials and only where the lifetime of the state involved allows the performance of vibrational motion can fine structure be expected. Most bands in the photoelectron spectra of complex molecules are broad and seemingly diffuse. This may be seen for tetrahydrofuran (figure 4) and may be related to the extensive fragmentation noted in the mass spectrum. Quite often, however, more particularly for simpler substances and those where extensive multiple bonding occurs for example in benzoquinone (figure 5*a*) and most notably for fluorinated compounds as in hexafluorobenzene (figure 5*b*) sharp fine structure arising from ionic vibrations is found. In just a few cases the graduation from ionic stability to instability can be seen to be reflected in a change in the photoelectron spectrum analogous to the 'breaking off' of fine structure common in optical spectroscopy.

The simplest example is provided by hydrogen (figure 6*a*) where lines converging towards a dissociation limit are succeeded by a weak continuum.

In hydrogen cyanide (figure 6*b*) instability arises from the possibility of radiationless transition between one ionic state which is initially stable and another which is immediately unstable at an energy level marked by the disappearance of fine structure. This also corresponds to the appearance potential of a fragment. A similar correspondence between such a discontinuity and a new fragmentation process is seen in water and sulphur hexafluoride (figure 6*c*). In formic acid (figure 6*d*) the appearance of the fifth band suggests that dissociation line broadening occurs at about 17.4 eV.

'Lone pair' electrons

The dissociative lifetime limitation to line width cited above may be expected to vanish for electron ejection from molecular orbitals whose spatial coordinates are those appropriate to the classical 'inert pair' of elementary electronic valence bond theory provided that the ion formed is then in its ground electronic state. According to Koopmans's theorem the positive hole achieves no redistribution in the vicinity of neighbouring bonds and no dimensional change can occur on ionization.

The number of examples other than in atoms at present known in which the first ionization process is the loss of such a 'lone pair' electron is remarkably small however; just water and the halogen acids and simple alkyl halides (other than fluorides). We may suspect that in general lone pair electrons may not be the most loosely bound and then their ejection, giving an ion in a configurationally excited state, may lead by curve crossing to rapid dissociation. In spite of this there are a number of examples where sharp lines (of width about equal to kT) in photoelectron spectra indicate the production of stable, undistorted ionic states which we can thus regard as due to lone pair ionization.

Cyanides and isocyanides

It is suspected that in hydrogen cyanide (figure 6*b*) and π and $2p\sigma_N$ electrons have a similar ionization energy. They are not clearly distinguished in the p.e. spectrum. The structure in the first band is complex but some of this complexity may also arise from Renner–Teller splitting of the degenerate π ionic states. In alkyl and aryl cyanides however this accidental degeneracy

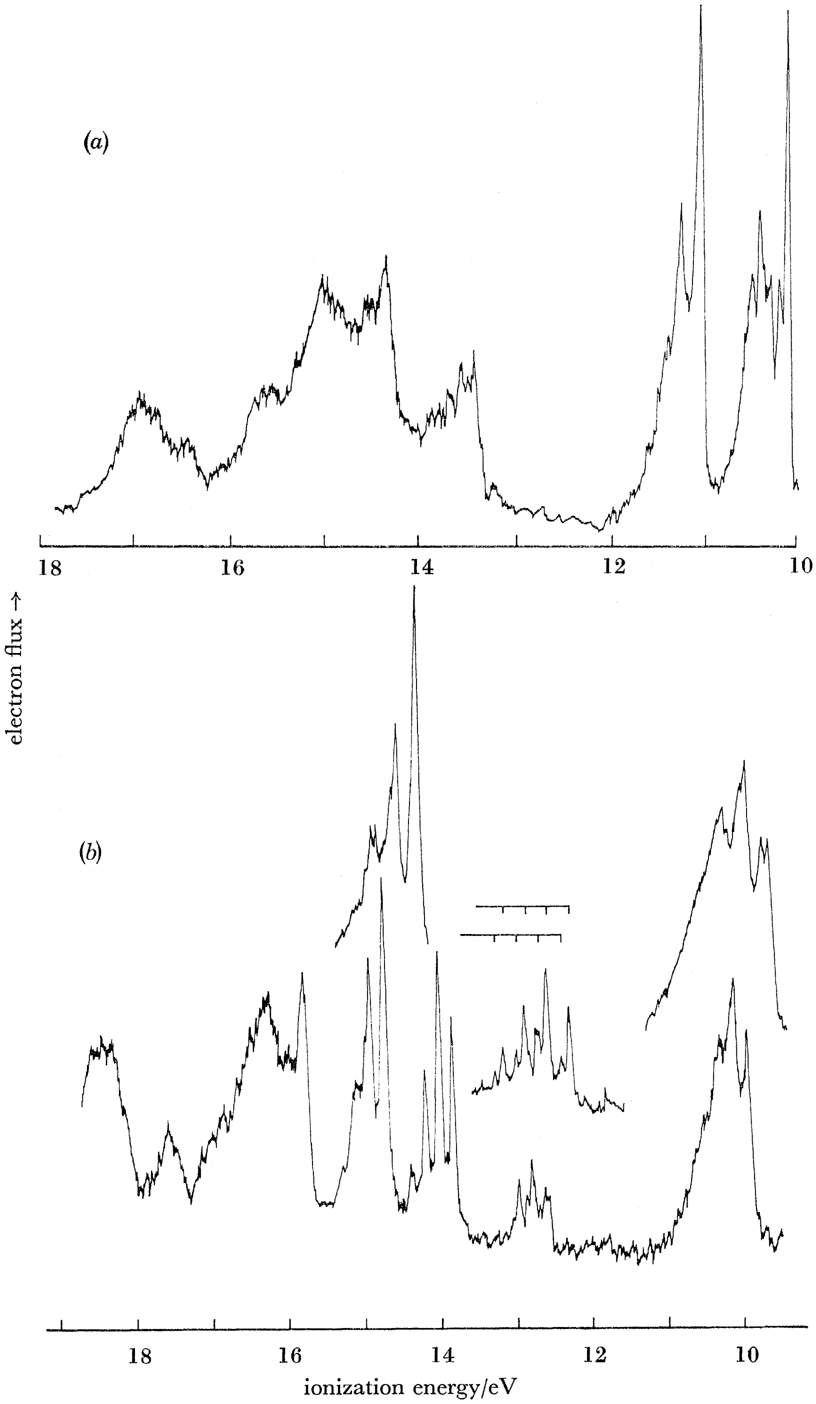

FIGURE 5. The helium 584 Å photoelectron spectra of (*a*) benzoquinone and (*b*) hexafluorobenzene.

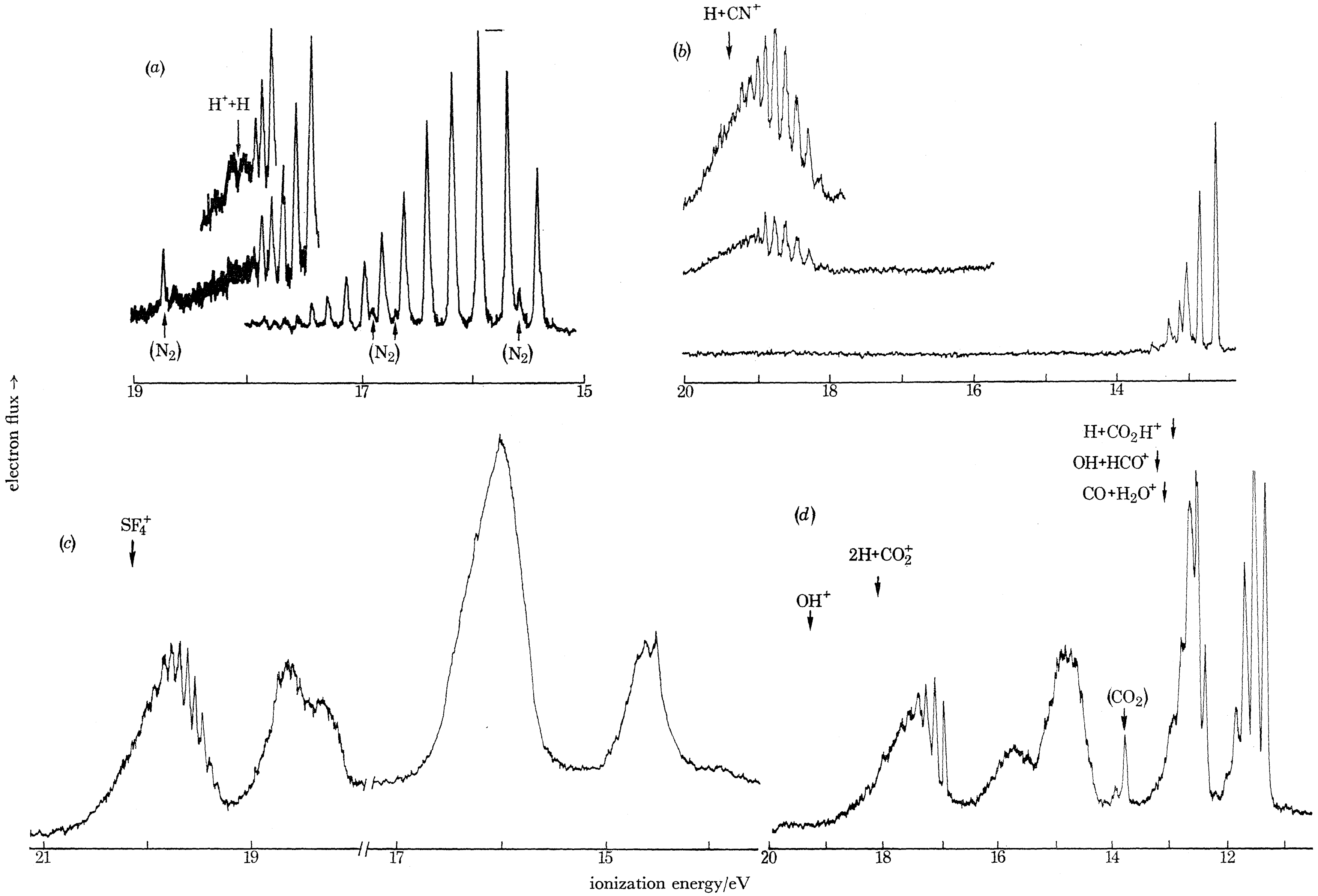

FIGURE 6. The helium 584 Å photoelectron spectra of (*a*) hydrogen, (*b*) hydrogen cyanide, (*c*) sulphur hexafluoride and (*d*) formic acid. Appearance potentials for the formation of ionic fragments are marked by arrows.

is removed and a separate sharp band can usually be distinguished near 13 eV (13.14 eV in CH_3CN) ascribable to the $2p\sigma_N$ orbital (5σ in HCN). In methyl cyanide (figure 7) some small C—H bonding character is indicated by the weak excitation of a vibration having a frequency of 1290 cm^{-1}. Since this is reduced to 970 cm^{-1} in CD_3CN ($\nu_H/\nu_D = 1.33$) it probably corresponds to the symmetric C—H deformation mode ν_3 (1376 cm^{-1}) of the molecule. The same assignment

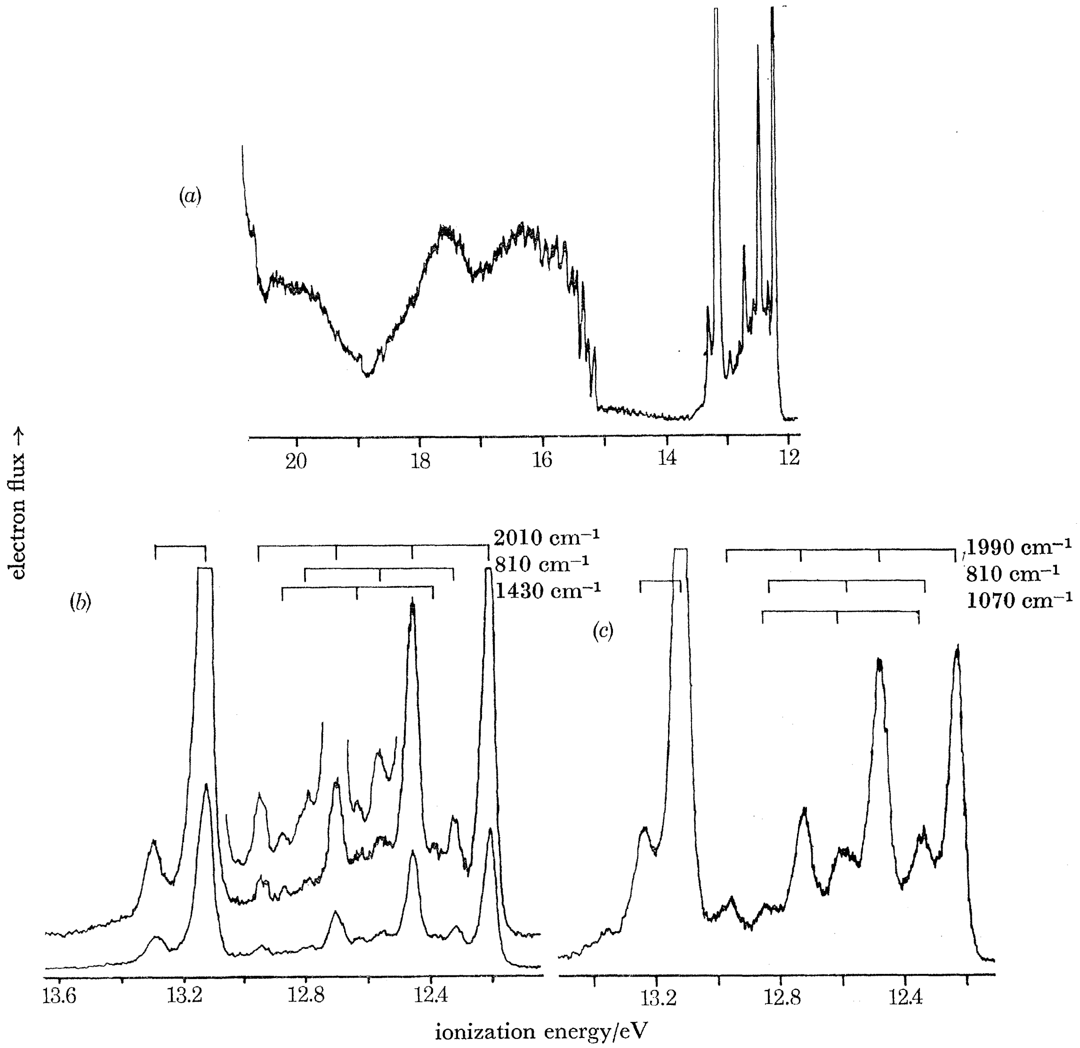

FIGURE 7. The helium 584 Å photoelectron spectrum of methyl cyanide: (*a*) full spectrum; (*b*) the high electron energy each to an expanded scale; (*c*) trideuteromethylcyanide as in (*b*).

may be made for a weak vibration (1410 cm^{-1}) accompanying the only sharp band in the methyl isocyanide spectrum (figure 8). The lone pair here must be essentially $2p\sigma_C$. An additional vibrational interval of 2880 cm^{-1} which can also be detected however indicates some $C \leftrightarrow N$ antibonding character since this can only be compared with the slightly lower frequency 2280 cm^{-1} in the molecule which is ν_2, the $C \equiv N$ stretching vibration.

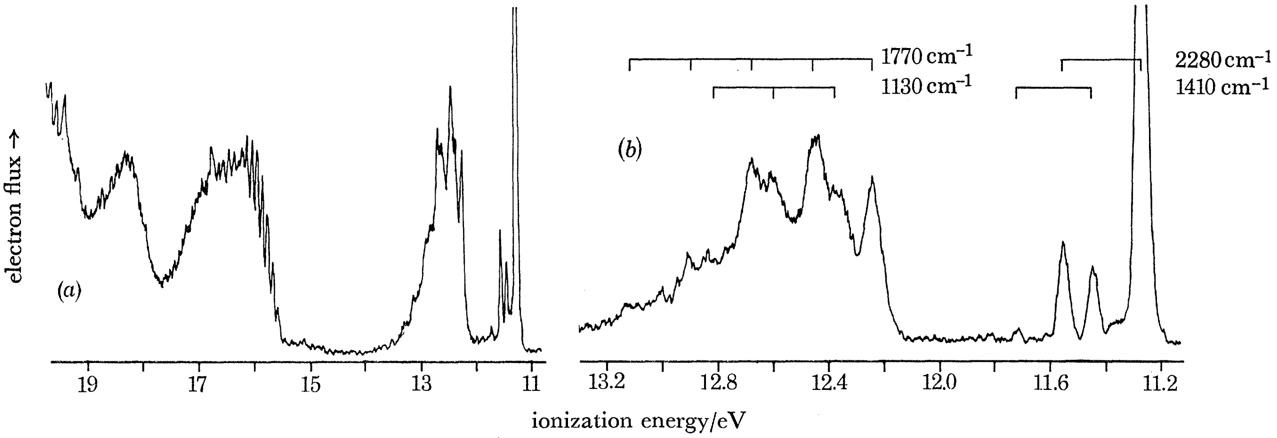

Figure 8. The helium 584 Å photoelectron spectrum of methyl isocyanide.

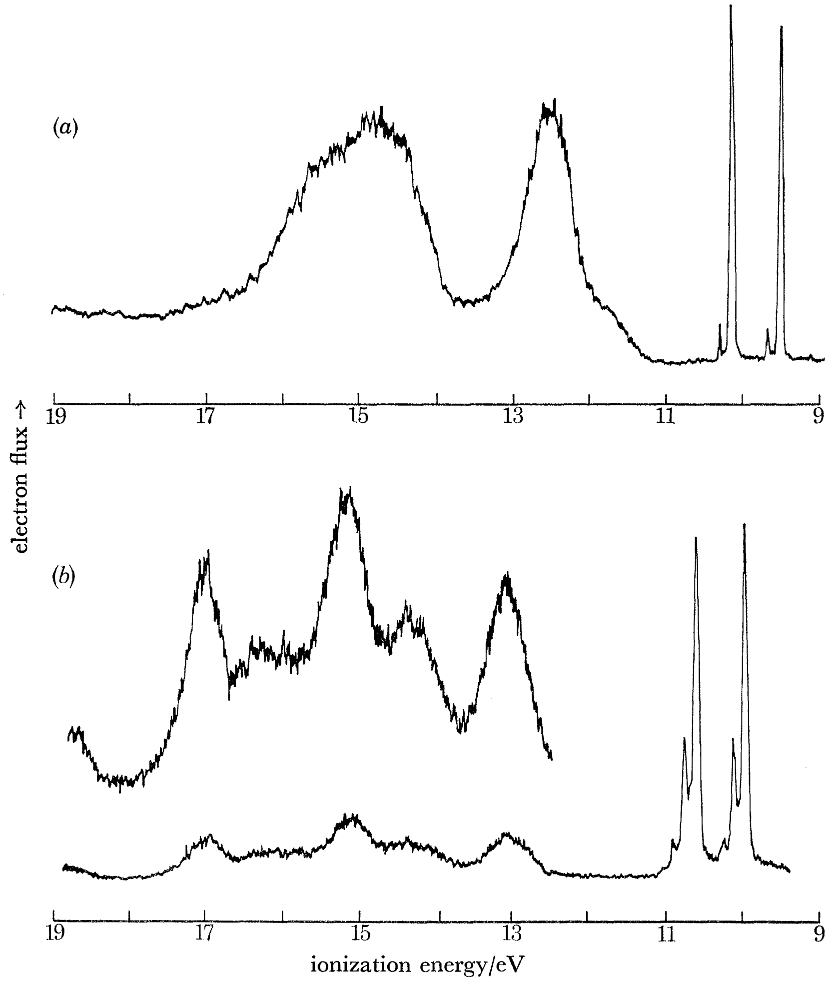

Figure 9. The helium 584 Å photoelectron spectra of (a) methyl iodide, (b) 2,2,2-trifluoroethyl iodide.

Halogenated compounds

Photoelectron spectra of compounds having halogen atoms usually show one or more fairly sharp bands. For monohalogen compounds more than 90 % of the halogen ionization transition probability may lie in the 0—0 component of what can sometimes be seen as a short progression in the halogen bond stretching frequency seen for example in methyl iodide (figure 9*a*). Such bands result from removal of one of the halogen 'lone pair' electrons which in the molecular ground state are in orbitals of an almost atomic character and which in molecules which are linear or have high enough symmetry are degenerate. The corresponding ions may thus show the effects of spin-orbit coupling in the doubling of the band, an effect which is small for monochlorides and vanishes in lower symmetry.

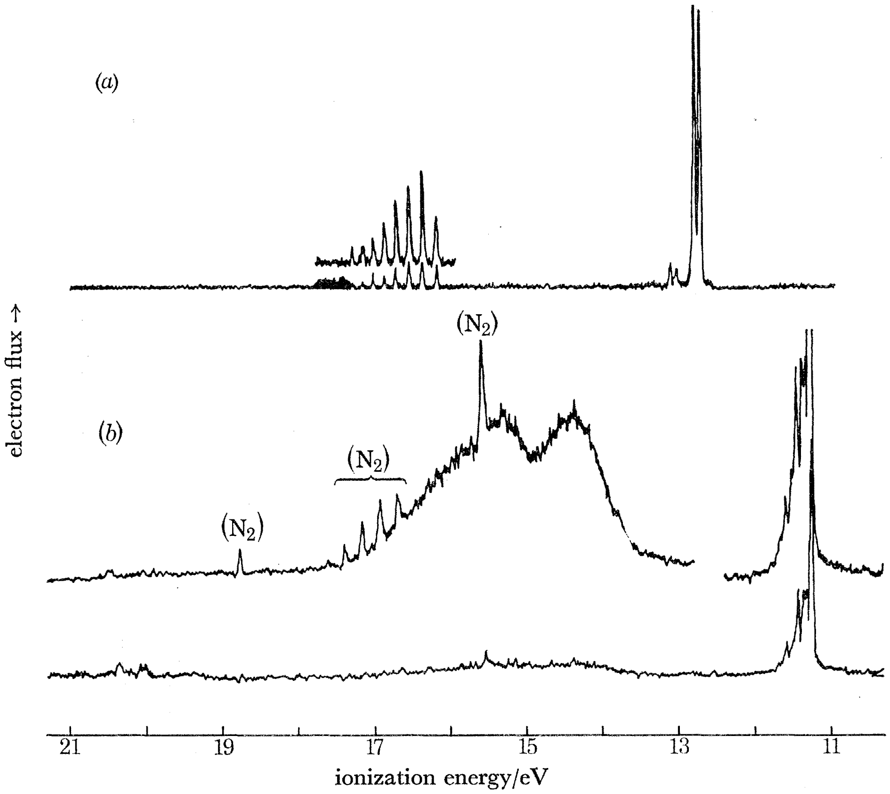

FIGURE 10. The helium 584 Å photoelectron spectra of (*a*) hydrogen chloride, (*b*) methyl chloride.

From the localized nature of the halogen npπ orbitals however only axial symmetry in the immediate vicinity of the halogen is important. Thus the iodine spin-orbit coupling persists in 2,2,2-trifluoroethyl iodide for example (figure 9*b*). Such insensitivity to lowering of symmetry is associated no doubt with the large spin orbit coupling parameter of the heavy atom but the relatively large size of the iodine atomic orbital compared with the molecular dimension is probably significant. The smaller coupling parameter and orbital size for chlorine restricts first order spin orbit splitting in photoelectron spectra to hydrogen chloride (figure 10*a*). Even in methyl chloride (figure 10*b*) the spin orbit coupling seems insignificant though the complexity of the fine structure suggests that it may be comparable in magnitude with Jahn–Teller splitting associated with the antisymmetric C—H deformation (see below).

In more complex monochloro-compounds a doublet structure is sometimes seen for which since it is often much larger than that expected for spin orbit coupling a different mechanism has been postulated (Baker, May & Turner 1968). This is seen when for example chlorine is attached to an olefinic or aromatic system. Chlorobenzene α-chloropyridine and α-chlorofuran are examples of this (figure 11*a*, *b*, *c*). In these cases the two lines differ in appearance, the

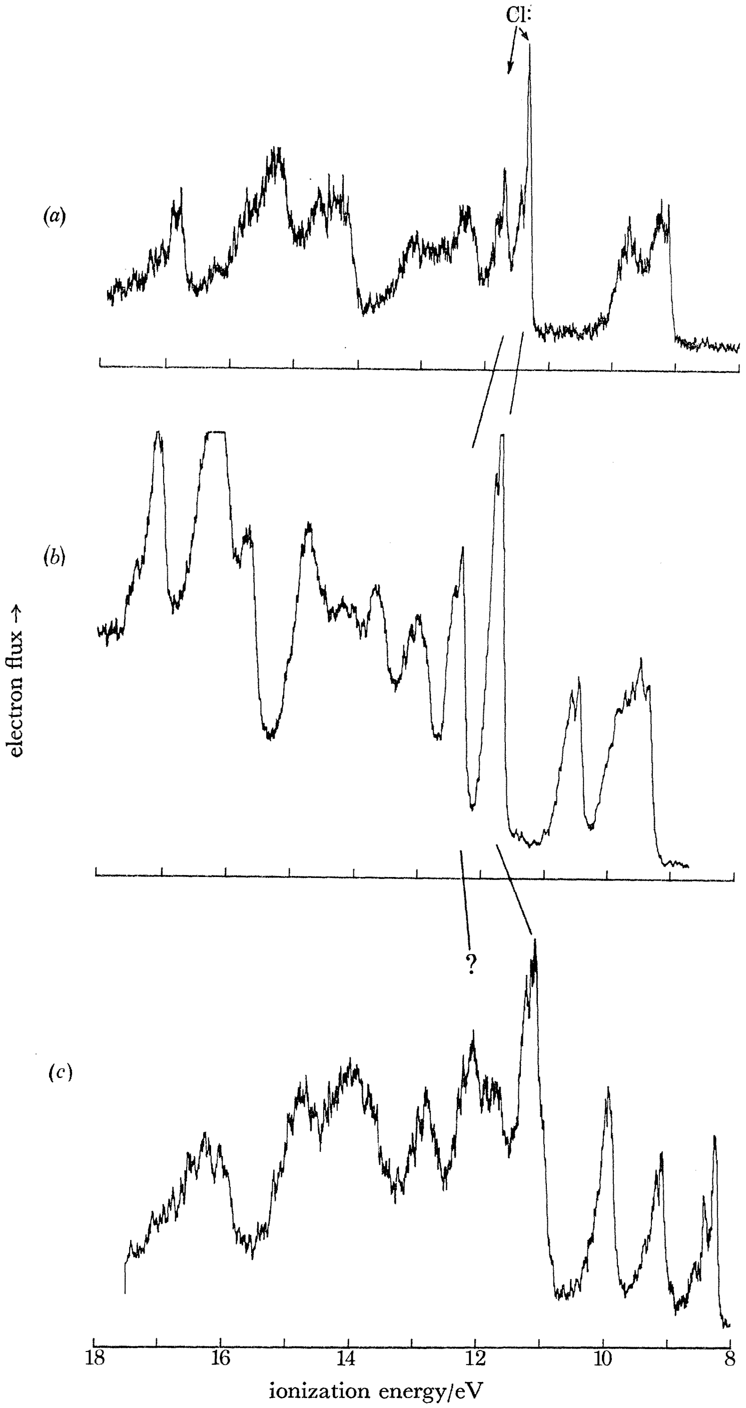

FIGURE 11. The helium 584 Å photoelectron spectra of (*a*) chlorobenzene, (*b*) α-chloropyridine and (*c*) α-chloronaphthalene.

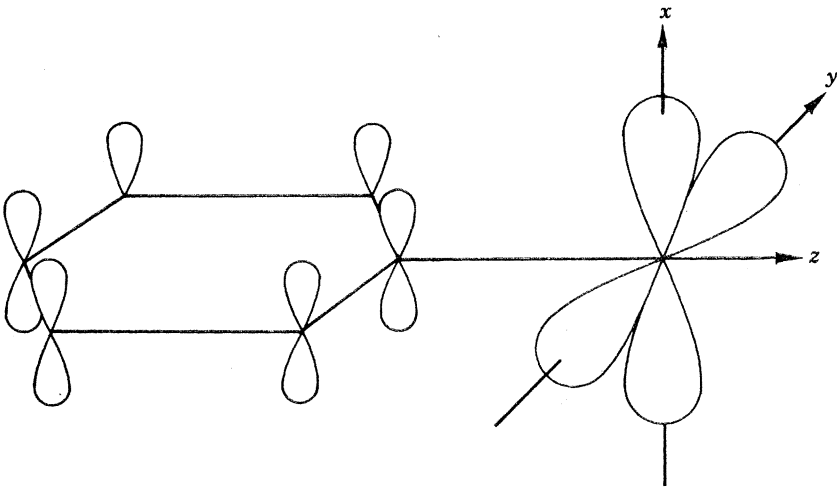

FIGURE 12. The orientation of the halogen np orbitals of halobenzenes in relation to the axes of the benzene ring.

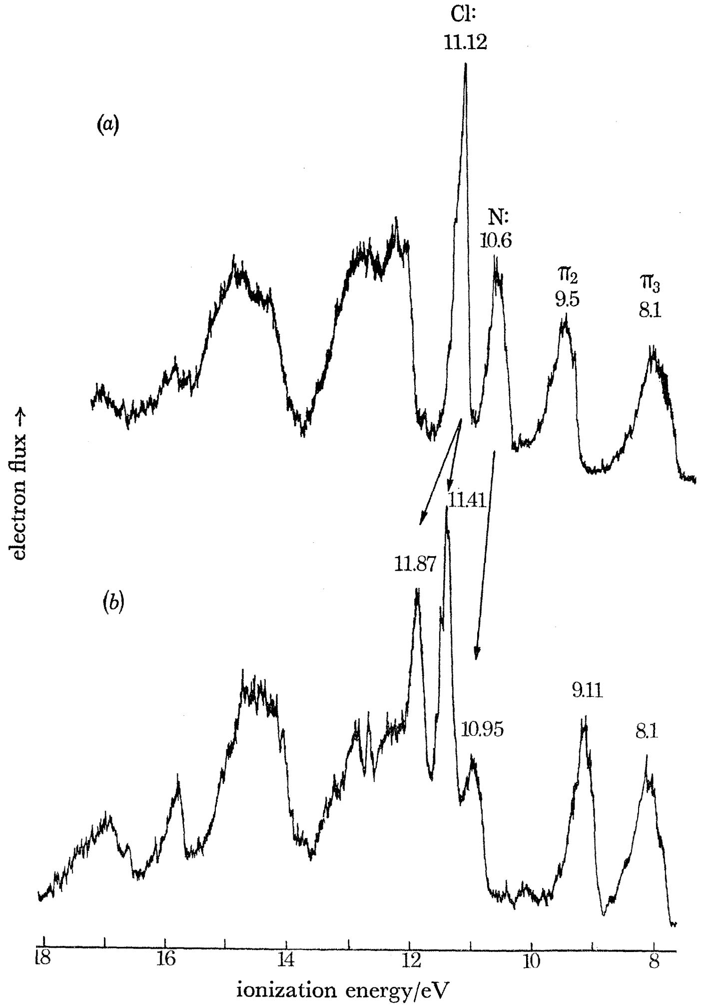

FIGURE 13. The helium 584 Å photoelectron spectra of (*a*) *p*-chloroaniline, (*b*) *o*-chloroaniline.

higher energy component being the 'sharper'. This may be associated with π–p interaction giving some C—Cl bonding character to the chlorine $3p_x$ atomic orbital (see figure 12), the $3p_y$ remaining essentially atomic in character suggesting that the ring σ orbitals with which it might mix are rather too low in energy.

We note that this last form of splitting seems to be extremely sensitive to changes in substituents where p–π delocalization is involved and vanishes in the presence of for example amino groups placed where p–π–p conjugation is greatest: in benzene the *para* position (figure 13*a*).

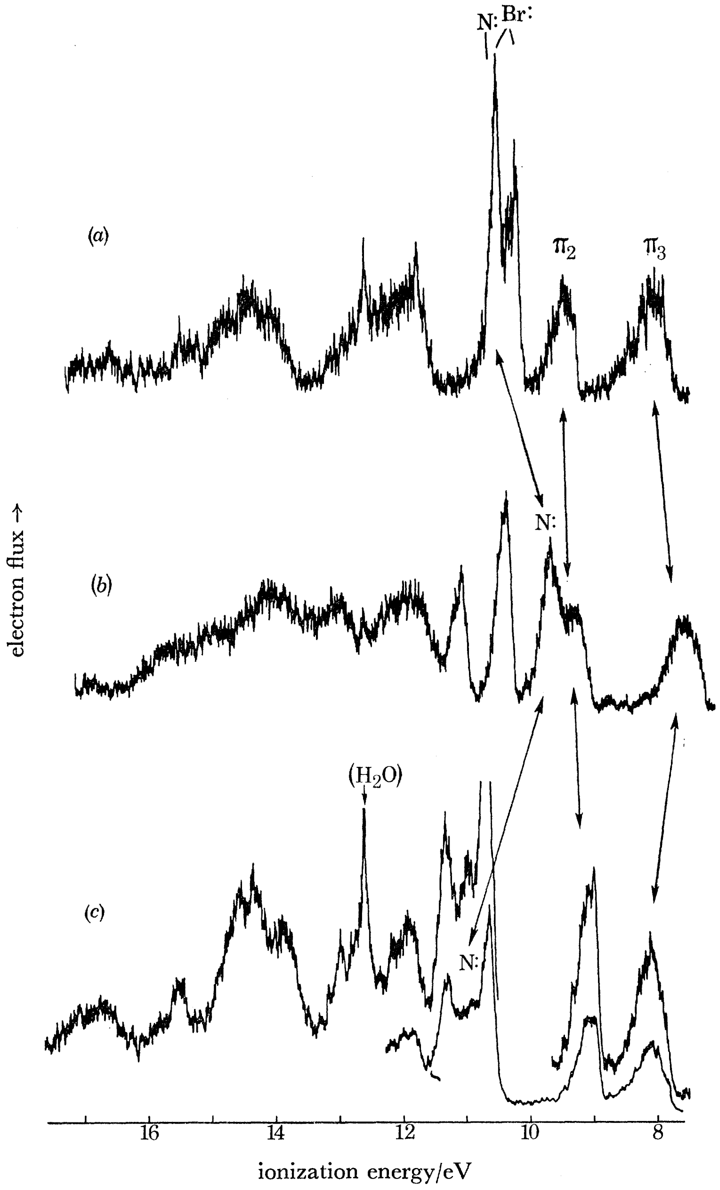

FIGURE 14. The helium 584 Å photoelectron spectra of (*a*) *p*-bromoaniline, (*b*) *p*-bromo-*N*,*N*-dimethylaniline, (*c*) *o*-bromoaniline.

Steric factors inhibiting resonance

In contrast to the *para* compound *o*-aminochlorobenzene (figure 13*b*) shows two well separated lines attributable to chlorine. It remains to be shown to what extent this is due to steric inhibition of resonance between the amino group and the ring. We find in *N*-alkylated *para*-bromoanilines however (figure 14*a*, *b*) clear evidence for such an effect. Again in the corresponding *ortho* compound (figure 14*c*) we see indications of a large proximity effect in the separation between the sharpest peaks (10.63 and 11.29 eV) which compare with that for diethylaminobromoaniline (10.29 and 10.96 eV).

The highest energy peak is again seen to be usually the sharpest and it can often be satisfactorily ascribed to a halogen p_y orbital. In chloro-compounds this seems generally a good approximation for the spin-orbit coupling may be neglected but in bromo-compounds it is less so. The energy of this band however should be affected most by interaction via σ orbitals. We can measure it very accurately feasibly to ±1 mV since it is usually so sharp and for *para*-substituents varying from cyano- to amino- the range is 0.78 eV (table 1).

The order we find is readily acceptable on chemical reactivity grounds as an inductive ($-I$) order. Quite small effects due to distant structural changes are readily measured as in the series where the *para*-substituent is —CHO (10.89 eV), —$COCH_3$ (10.78 eV) or —COC_2H_3 (10.77 eV): or again in the series *p*-CH_2CN (10.56 eV), —CH_3 (10.55 eV) or —C_2H_5 (10.49 eV). No clear correlation exists with the Hammet σ constants σ_p, σ_p^+ or σ_I though the σ_p values reflect the general trends most closely as might be expected.

TABLE 1. FIRST BROMINE 'LONE PAIR' IONIZATION ENERGY (SEE TEXT) AND HAMMETT σ CONSTANTS (MARCH 1968) FOR COMPOUNDS OF THE TYPE XOBr

X	$I_{Br'}$/eV	σ_p	σ_p^+	σ_I
—CN	11.03	+0.67	+0.66	+0.56
—NO_2	10.92	+0.78	+0.79	+0.63
—CHO	10.89	+0.45	—	+0.31
—F	10.81	+0.06	−0.07	+0.52
—COMe	10.78	+0.50	—	+0.28
—COPh	10.78	—	—	—
—COEt	10.77	—	—	—
—COPr	10.77	—	—	—
—H	10.60	0.0	0.0	0.0
—CH_2CN	10.56	—	—	—
—CH_3	10.53	−0.31	−0.31	−0.05
—Et	10.49	—	—	−0.05
—$CH:CH_2$	10.35	—	—	+0.05
—NMe_2	10.33	−0.17	−1.7	+0.10
—NEt_2	10.29	—	—	—
—OMe	10.29	−0.11	−0.78	+0.26
—CH_2Br	10.27	—	—	(+0.17—CH_2Cl)
—NH_2	10.25	−0.17	−1.3	+0.13

Amine-nitrogen and ether-oxygen 'lone pairs'

Though the water molecule is exceptional the photoelectron spectra of divalent oxygen and trivalent nitrogen compounds reveal no classical 'lone pairs'. Nevertheless, we can often identify a band with this feature from comparative studies between related structures. It is of course imprecise to speak of a nitrogen lone pair in aniline and especially in its ion; the nitrogen lone pair must be much delocalized by conjugation. The interpretation of the spectra of substituted anilines is assisted however by some such rationalization. This simplification helps with the counting of the energy levels. The band marked N, in figure 15*a*, *b*, *c*, can be followed through the series. Similarly, ether oxygen (figure 16*a*) gives rise to fairly narrow bands near 9.5 eV while in phenoxy compounds this feature is found near 10.5 eV (figure 16*b*). The carbonyl group in aldehydes and ketones leads to a band due to the oxygen 2p 'lone pair', between 9 and 11 eV. In unsubstituted aliphatic aldehydes and ketones this represents the first ionization potential. In carbocyclic aromatic compounds the band may be overlaid by one due to π ionization in the ring but may be located by following the effect of alkyl substitution (figure 17*a*, *b*, *c*).

Correlations between Franck–Condon factors, changes in vibrational frequencies, and the bonding type of the electron excited in transitions

It is interesting to see how the vibrational frequencies change from the molecule (X) to each of the ionic states (X), (A) ,(B) and (C) say.

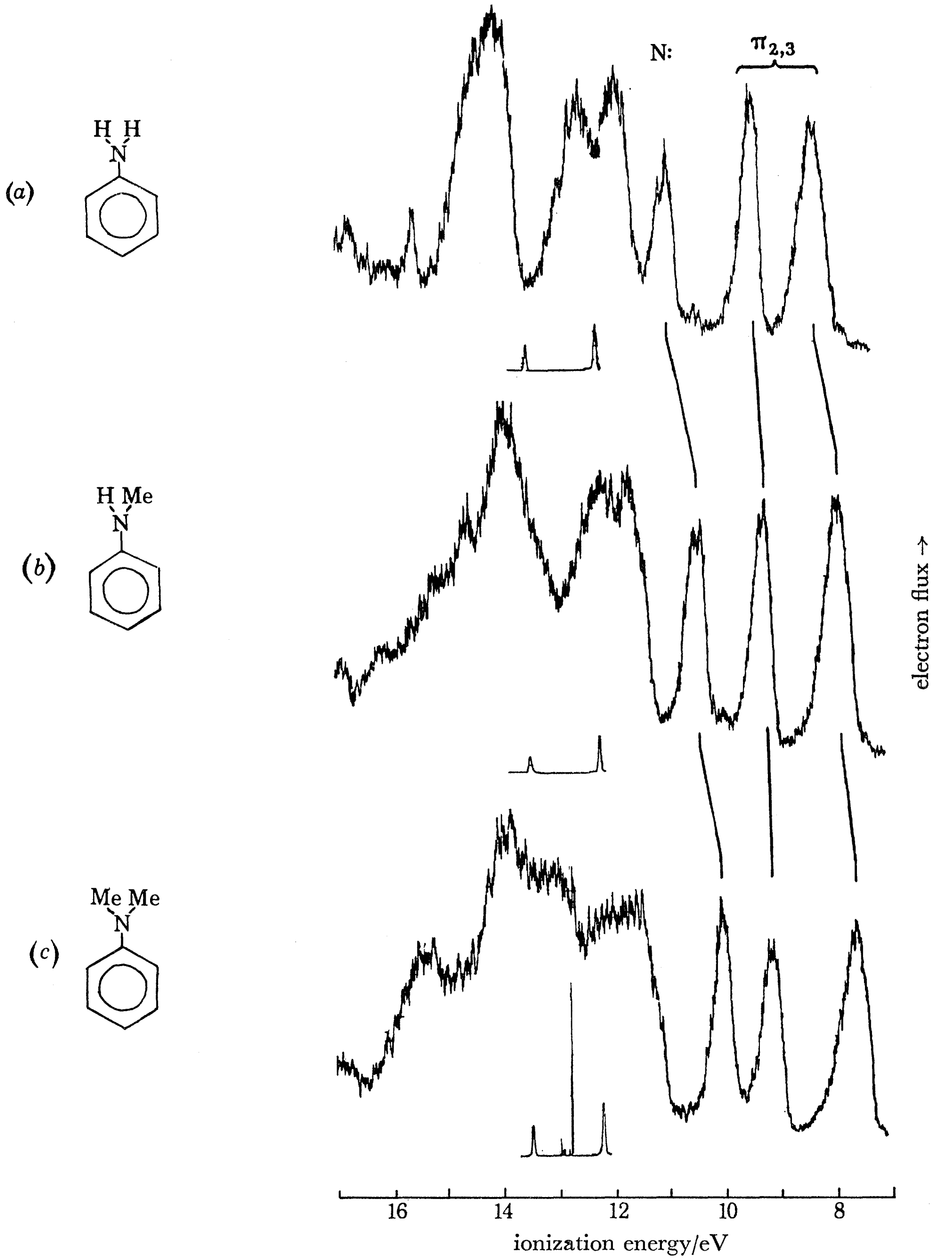

FIGURE 15. The helium 584 Å photoelectron spectra of (*a*) aniline, (*b*) *N*-methylaniline and (*c*) *N*,*N*-dimethylaniline.

The energies of the vibrational levels are given by

$$E_V = (v'+\tfrac{1}{2})\,h\omega-(v'+\tfrac{1}{2})^2\,h\omega x+\text{smaller terms}$$

where v' is the vibrational quantum number in the ion, h is Planck's constant, x is the anharmonicity constant, $\omega = \sqrt{(k/\mu')}/2\pi$, the vibrational frequency, k is the force constant of the vibration, μ is the reduced mass of the system.

Now k is a measure of the strength of the bond. If a non-bonding electron is removed on ionization, the bond strength will alter little, and so k, and hence ω and the energy separation between vibrational levels, will remain almost unchanged. The bond lenth r_e will also be unaffected. On removing a bonding electron, k and ω will decrease, and r_e will increase. Conversely, on removing an anti-bonding electron, k and ω increase and r_e decreases. Similar effects occur when the electron is just excited to a higher molecular level and not completely ionised.

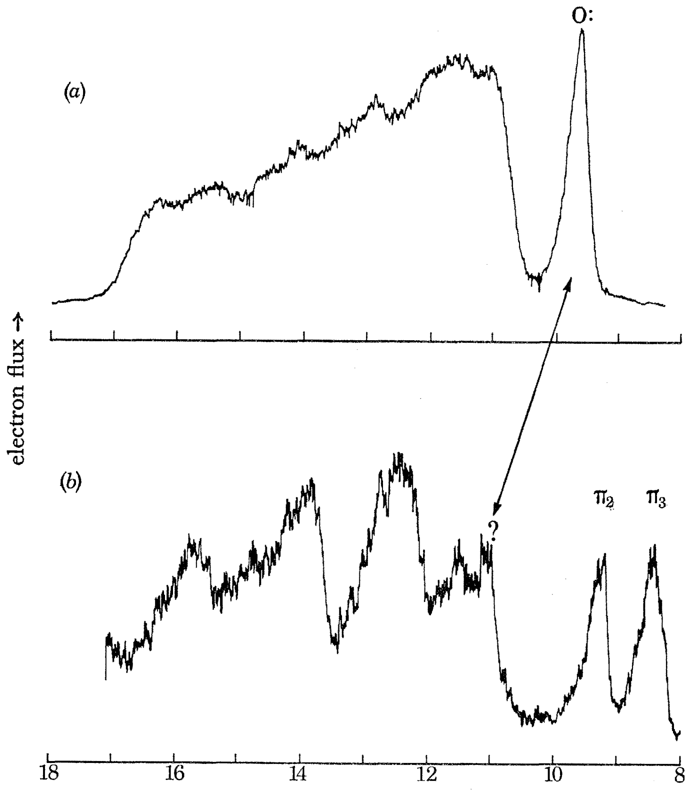

FIGURE 16. The helium 584 Å photoelectron spectra of (a) methylbutyl ether, (b) anisole.

Since the values of the Franck–Condon factors are dependent on r_e they will also be characteristic of the bonding character of the electron removed. Removal of non-bonding electrons leads to transitions essentially to the $v' = 0$ level, while bonding or anti-bonding electrons will significantly populate higher v' levels, so that the maximum Franck–Condon factor may not be that for $v' = 0$. This argument can be extended to cover polyatomic systems but in practice it becomes complex because even for linear triatomic molecules three vibrational modes are involved and a three-dimensional potential surface is required to describe correctly the vibrational motion of the molecule.

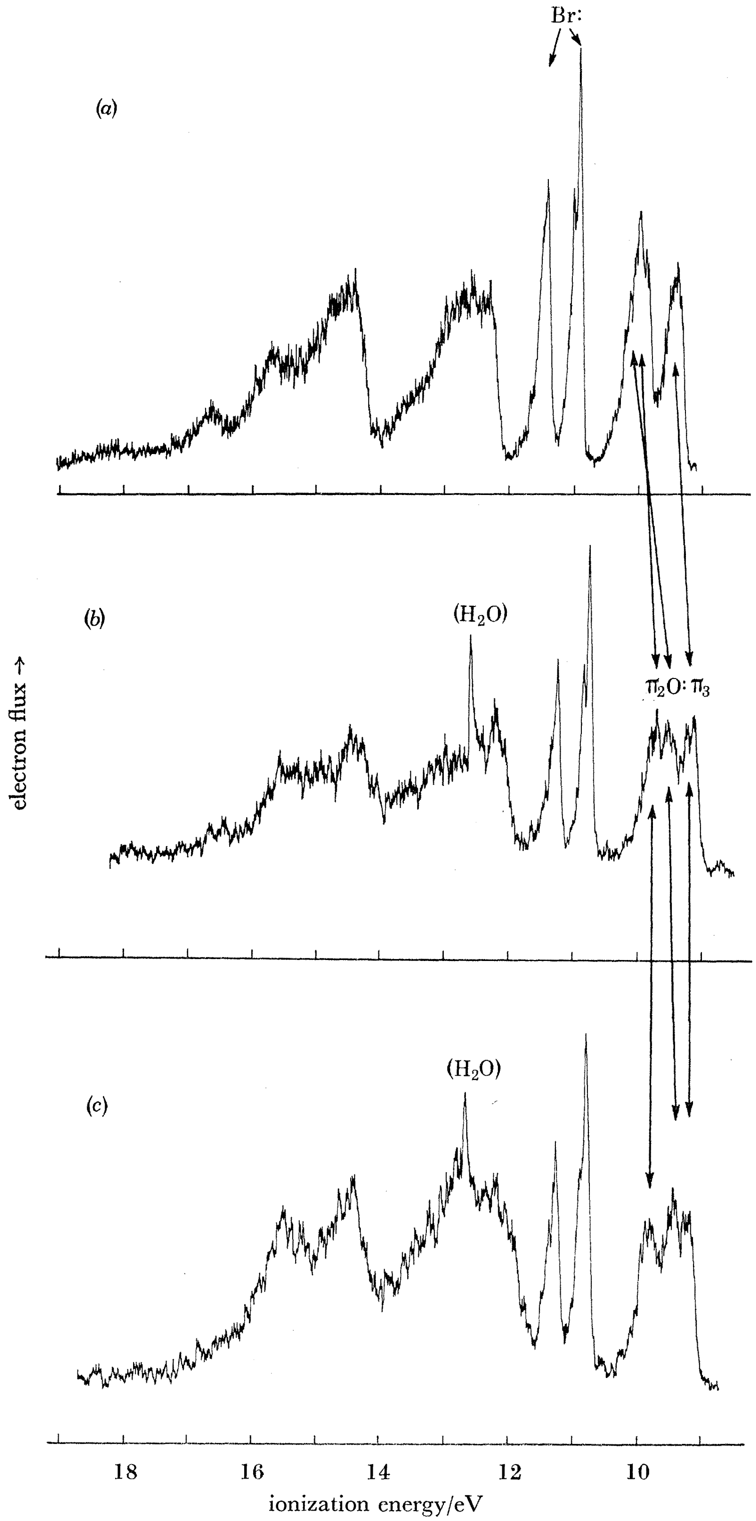

FIGURE 17. The helium 584 Å photoelectron spectra of (*a*) *p*-bromobenzaldehyde, (*b*) *p*-bromoacetophenone and (*c*) *p*-bromopropiophenone.

It is of some interest nevertheless to see whether or not some practical use may be made of the vibrational fine structure which is observable even for polyatomic molecules. To do this we must assign the vibrational intervals to modes of vibration appropriate to the ionic symmetry which may be assumed to be related, perhaps closely, to that of the molecule.

In optical spectroscopy there are a number of well-known empirical relations linking the internuclear distance r_e and the vibrational frequency (*a*) in different electronic states of the same diatomic molecule and (*b*) in a related series of molecules. The reader is referred to Herzberg (1950) for a more complete discussion of the various 'rules'. We may extend case (*a*)—different electronic states of the same molecule—to include the ionic states by using Mecke's relation:

$$\omega_e \propto r_e^{-2}.$$

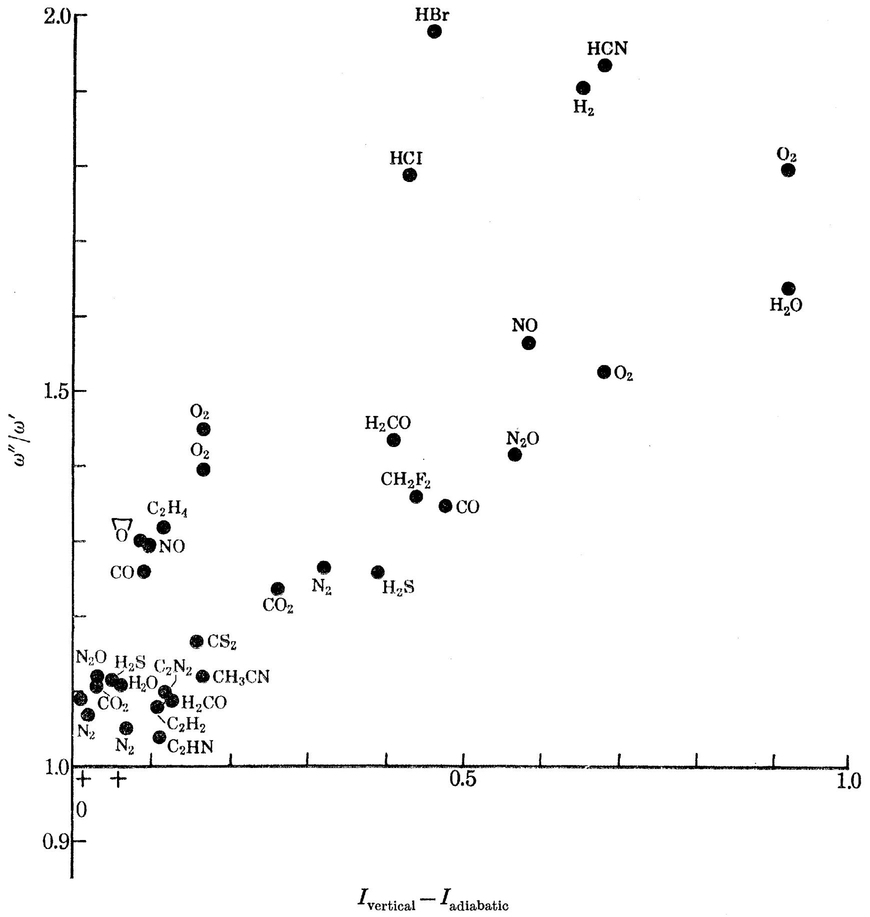

FIGURE 18. The relation between the adiabatic–vertical ionization energy difference ΔE and the change in vibrational frequency on ionization ω''/ω' (see text).

For small changes in r_e we may assume the potential function to be approximately parabolic so that the difference ΔE between the adiabatic and vertical ionization energies I_V—I_A which is in general a function of the fractional change in internuclear distance may be expressed as:

$$\Delta E = I_V - I_A = A[(r'/r'')^2 - 1].$$

Hence from Mecke's relation we expect:

$$\Delta E = I_V - I_A = A[(\omega''/\omega') - 1].$$

This has been tested using examples about whose vibrational assignments there is no ambiguity and the results are summarized in figure 18. It would appear that though there is in fact some agreement with the expected linear relation some grouping near two curves is apparent. For the main branch $A \approx 1.2$. From measured vertical–adiabatic ionization potential difference therefore it may be possible in favourable cases to infer to what molecular vibrational mode an observed ionic frequency corresponds.

Examples

In methyl fluoride (figure 19*a*) the molecular modes of vibration are as follows:

ν_1	ν_2	ν_3	ν_4	ν_5	ν_6
2964	1475	1048	2892	1471	1195
C↔H (s)	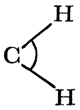 (s)	C↔F	C↔H (a)	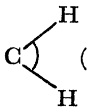 (a)	

For the progression in the first band $\Delta G = 0.132$ eV ($1080\ \text{cm}^{-1}$) and $\Delta E = 0.35$ eV, so that $\omega''/\omega' = 1.3$. We conclude that the vibration excited corresponds to ν_2 since the predicted value of ω'' is $1400\ \text{cm}^{-1}$. The C—F stretching frequency if excited would not be expected to lead to a long progression ($1070\ \text{cm}^{-1}, \leftarrow 1048\ \text{cm}^{-1}$).

In difluoroethylene the progression in the first band (figure 19*b*) has $\Delta G = 0.18$ eV ($1450\ \text{cm}^{-1}$). Here we need only consider the first four molecular modes of vibration ν_1–ν_4 as ν_5 to ν_{12} are all lower in frequency.

ν_1	ν_2	ν_3	ν_4
3101	1728	1359	915
C↔H	C↔C	CH_2(def.)	C↔F

Again ΔE is 0.55, $\omega''/\omega' = 1.3$ and we deduce that $\omega'' \approx 1880$, that is ν_2, the double bond stretching frequency. Here it seems clear that the alternative possibility of an increase in ν_3 ($1450 \leftarrow 1359$) is excluded by the large value of ΔE but such a possible ambiguity may arise in other cases.

Similar reasoning leads to the assignment of a vibration in the state of SF_6^+ near 19.5 eV (figure 19*c*) to ν_3. In ketene (figure 23) well resolved vibrational fine structure appears in three bands. In the first we can assign it to two modes (ν_2 and ν_4, respectively antisymmetric and symmetric stretching modes). The third and fourth bands through differeing markedly in appearance receive the same assignment namely to ν_3 the symmetric hydrogen deformation. Similarly, the first two bands in the pyrazine spectrum though having very different Franck–Condon envelopes can receive the same assignment (figure 20) ν_4 the ring breathing mode for the main vibrational interval. In the third band the ring stretching mode ν_2 is indicated.

Energy level diagrams

Inspection of the photoelectron spectra for compounds that are members of a series related by common electronic structural features (for example iso-electronic series) frequently reveals marked resemblances particularly in the shapes of selected bands. That is to say the Franck–Condon envelopes of bands arising in the ionization of electrons from orbitals whose symmetry properties, and l.c.a.o. coefficients provide by their apparent invariance a means of identification.

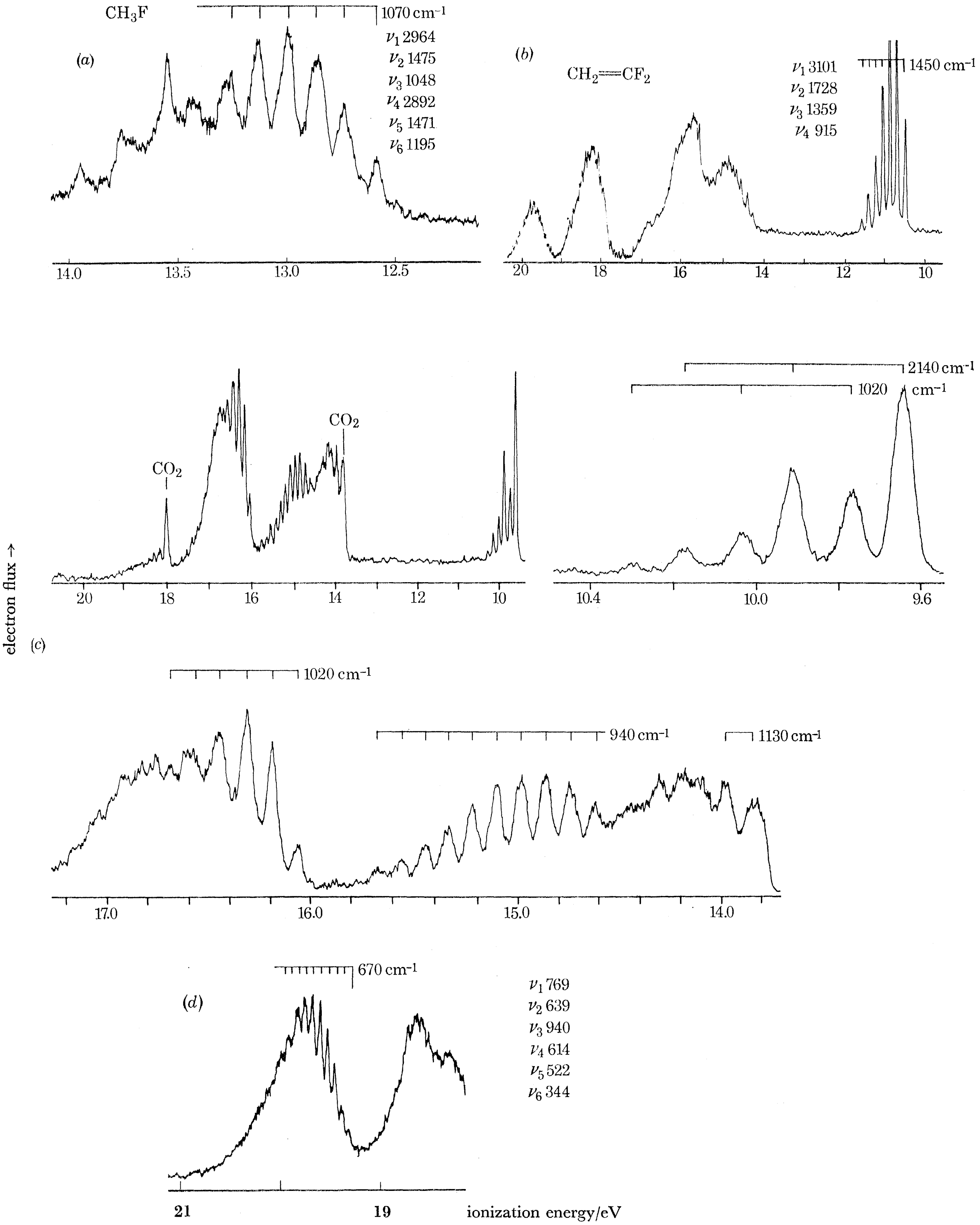

FIGURE 19. Portions of the helium 584 Å photoelectron spectra of (*a*) methyl fluoride, (*b*) 1,1-difluoroethylene, (*c*) ketene and (*d*) sulphur hexafluoride. The relevant molecular vibrational frequencies are shown for comparison (see text).

This takes on greater precision when the vibrational fine structure exhibits demonstrably common features as between the same band observed in the spectra of different substances.

In one particular band of the spectra of diacetylene, cyanoacetylene and cyanogen for example the marked resemblance between the second, third and third bands respectively is due to their containing vibrational fine structure in the form of two short, overlapping progressions one, the shorter, in the triple bond stretching frequency ν_1:

$$\leftarrow \mathrm{X{\equiv}C} \rightarrow\!\leftarrow \mathrm{C{\equiv}X} \rightarrow \quad (\mathrm{X = N \text{ or } CH}),$$

and the other extending up to about $v' = 4$ in ν_2 the C—C single bond stretching frequency:

$$\leftarrow \mathrm{X{\equiv}C} \longleftrightarrow \mathrm{C{\equiv}X} \rightarrow.$$

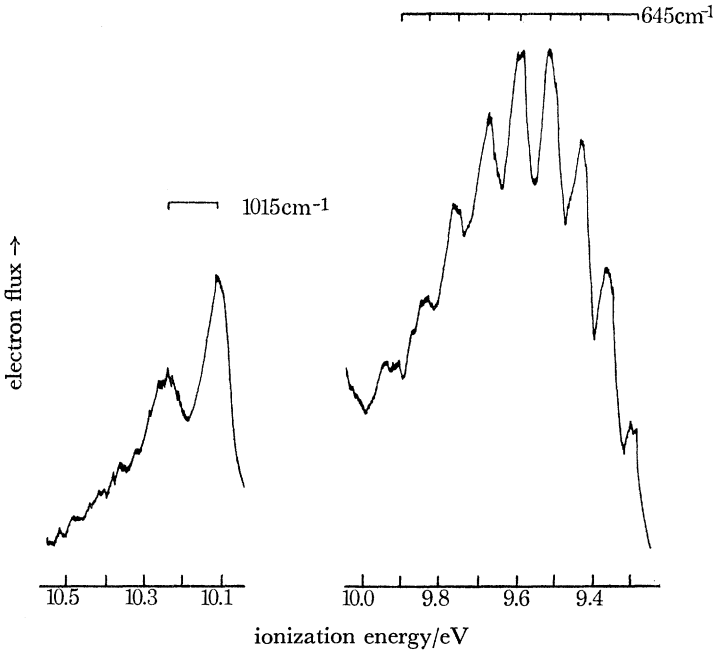

FIGURE 20. Part of the helium 584 Å photoelectron spectrum of pyrazine (see text).

The energy level diagrams that we find can be seen to be strictly speaking ionic energy level diagrams showing the relative energies of different ionic configurations compared to the ionic ground state. These would normally be plotted upside down, excited configurations then appearing above the ground state configurations. If we adhere to the form of a conventional molecular orbital energy level diagram (and ignore by implication deviation from Koopmans's theorem) the salient features associated with, for example, electronegativity changes on the introduction of heteroatoms have immediate chemical significance. This approach helps the interpretation of the spectrum of butadiene, acrolein and glyoxal for these bear a relation to one another similar to that among the members of the series diacetylene, cyanoacetylene and cyanogen. The dominant effect of heteroatom replacements is seen through the medium of the experimental energy level diagram (Baker & Turner 1968). An effect closely similar in magnitude is seen in the present series and enables us to identify the π_u and π_g levels with some confidence and to relate them in turn to ethylene and formaldehyde. The constancy of the π_u, π_g separation in both series is noteworthy. It is a measure of the CC resonance integral. There is a similarity in the vibrational fine structure which is only really obvious in glyoxal but here the dominant vibration in both π_u and π_g levels is the multiple bond stretching mode ν_3 an assignment based on the ΔE; v''/v' correlation given above and summarized as follows:

p.e. band	ΔG	ΔE	ω''/ω'	ω'' (calc.)
2	1610	0.14	1.08	1740 cm^{-1}
3	1360	0.31	1.26	1710 cm^{-1}

ν_1	ν_2	ν_3	ν_4	ν_5	ν_6	ν_7	ν_8	ν_9
2844	2836	1745	1730	1338	1312	1060	550	341
(s) C↔H (a)		(s) C↔O (a)		(s) C—H (a)		C↔C	(s) C C O (a)	

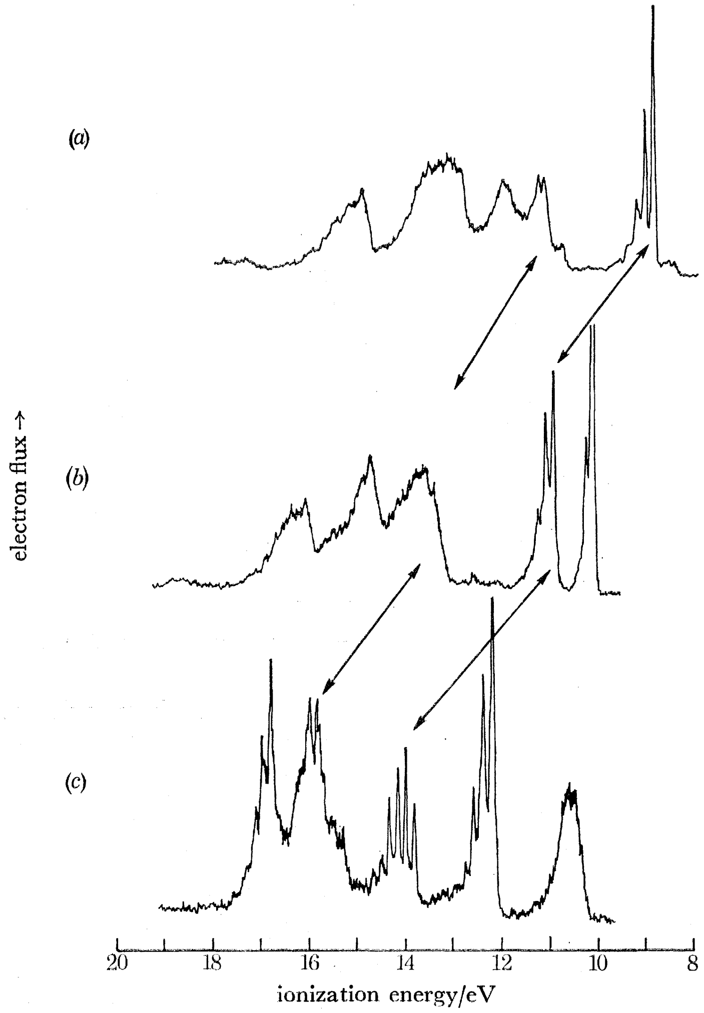

FIGURE 21. The helium 584 Å photoelectron spectra of (*a*) butadiene, (*b*) acrolein and (*c*) glyoxal. The π_u and π_g ionizations are linked (see text).

This paper is based for the most part upon work at Imperial College, London and the University of Oxford by J. B. Atkinson, A. D. Baker, C. Baker, C. R. Brundle, M. I. Al-Joboury, D. P. May and T. N. Radwan.

REFERENCES (Turner)

Baker, A. D., Baker, C., Brundle, C. R. & Turner, D. W. 1968 *J. Mass Spectr. Ion Phys.* **1**, 285.
Baker, A. D., May, D. P. & Turner, D. W. 1968 *J. chem. Soc.* p. 22.
Baker, C. & Turner, D. W. 1968 *Proc. Roy. Soc. Lond.* A **307**, 27.
Baker, C. & Turner, D. W. 1969 *Chem. Commun.* p. 480.
Basch, H., Robin, M. B., Kuebler, N. A., Baker, C. & Turner, D. W. 1969 *J. chem. Phys.* **51**, 42.
Collin, J. E. & Natalis, P. 1968 *J. Mass Spectr. Ion Phys.* **1**, 121.
Herzberg, G. 1950 *Molecular structure and molecular spectra. I. Spectra of diatomic molecules.* p. 456. New York: D. Van Nostrand.
Al-Joboury, M. I., May, D. P. & Turner, D. W. 1965 *J. chem. Soc.* p. 616.
Klemperer, O. 1965 *Rept. Progr. Phys.* **28**, 77.
Longuet-Higgins, H. C., Öpik, U., Pryce, M. H. L. & Sack, R. A. 1958 *Proc. Roy. Soc. Lond.* A **244**, 1.
March, J. 1968 *Adv. Org. Chem.* p. 231.
Price, W. C. 1968 *Molecular spectroscopy* (ed. P. W. Hepple). London: the Institute of Petroleum, New York: Elsevier.
Samson, J. A. 1969 *Rev. Scient. Instrum.* **40**, 1174.
Turner, D. W. 1968 *Proc. Roy. Soc. Lond.* A **307**, 15.
Turner, D. W. 1970 *Molecular photoelectron spectroscopy.* London: Interscience.
Turner, D. W. & Al-Joboury, M. I. 1962 *J. chem. Phys.* **37**, 3007.
Watanabe, K. 1959 *J. chem. Phys.* **26**, 542.
Weissler, G. L. 1956 *Handbuch der Physik* (ed. Flugge), **21**, 304 ff. Berlin: Springer-Verlag.